

Shape reconstruction based on FBG flexible sensor*

WANG Yan**, XU Haoyu, JIN Ping, WANG Junliang, and ZHU Wei

School of Electrical and Information Engineering, Anhui University of Technology, Maanshan 243000, China

(Received 17 January 2022; Revised 20 April 2022)

©Tianjin University of Technology 2022

In this paper, the shape of the object is reconstructed based on the fiber Bragg grating (FBG) flexible sensor encapsulated by polydimethylsiloxane (PDMS) material, and the influence of the number and layout of the sensors on the reconstruction accuracy of the object is studied. The COMSOL simulation software is used to verify the accuracy of the algorithm, and four sensors are prepared to measure and reconstruct the bent aluminum plate under set conditions. The maximum relative error of the shape reconstruction span is 1.203%, and the maximum relative error of the height is 2.802%. The research results provide the application basis for the shape detection of soft robots.

Document code: A **Article ID:** 1673-1905(2022)08-0454-7

DOI <https://doi.org/10.1007/s11801-022-2005-x>

The traditional industrial rigid manipulator has many problems, such as inflexible movement and poor obstacle avoidance performance, while the flexible manipulator has a degree of freedom far greater than the number of degrees of freedom necessary to perform tasks. Therefore, it has good bending characteristics and movement flexibility, and has gradually been widely used in disaster rescue robots, medical surgical robots and nuclear power plant robots. It is one of the most important frontier development directions in the current robotics field.

However, because flexible manipulator has infinite degrees of freedom and no concept of "joint" in theory, the traditional kinematic/dynamic model of rigid manipulator can't be applied, and the flexible material on the surface is too sensitive to external disturbances, resulting in unstable shape and difficult to be estimated. Therefore, under the situation without accurate modeling, if the terminal positioning control and compliance control are accurately realized, it is necessary to achieve high-precision shape detection, so as to sense and respond to the surrounding environment for the flexible robot and provide state feedback to the controller.

At present, sensors which are commonly used in the shape perception of objects include laser sensors^[1], capacitive sensors^[2] and piezoresistive tactile sensors^[3], etc. Laser sensors can't be used in harsh environments. Capacitive sensors and piezoresistive sensors on flexible materials may cause inaccurate detection due to poor compatibility.

Optical fiber sensors have the advantages of small size, light weight, simple structure, high sensitivity, and fast response speed, and have high sensitivity and strong anti-interference in harsh environments, which makes

optical fiber distributed sensors widely applied in the field of soft robots. YAN et al^[1] proposed a plate structure deformation monitoring system based on quasi-distributed fiber grating sensor network and a coordinate conversion surface reconstruction algorithm, so that the root mean square error of the deformation of the measurement point is no more than 0.04 mm, and the relative error is no more than 3.5%. GUO et al^[4] proposed a flexible sensor based on double-layer orthogonal fiber Bragg grating (FBG) that can realize 3D shape measurement, and the curvature measurement error for complex surfaces is only 2.8%—4.5%. YANG et al^[5] designed a soft robotic gripper with sinusoidal embedded stretchable FBG sensor, which can sense and respond to its surrounding environment and provide its operating status to the controller, and the sensitivity is increased by 7 times. ISMAIL et al^[6] developed a novel 3D printed dual-axis sensor system for tilt measurement based on four FBG devices and demonstrated its highly linear response over a tilt range of 0±90°. GROVES et al^[7] proposed a multi-mode optical fiber sensing measurement method to study the trailing edge deflection of the SmartX camber deformable wing demonstrator, and proved that under the condition of 2.8 mm deflection accuracy, the error is only 9%.

FBG has been studied extensively in object shape perception, but there is still some space to be studied in sensor layout in FBG sensing process. In this paper, the concept of FBG flexible sensor based on polydimethylsiloxane (PDMS) material as the fiber grating package substrate is proposed, and the relationship between the center wavelength shift of the fiber grating due to the bending of the contact object and the curvature of the

* This work has been supported by the Provincial Science and Technology Major Project of Anhui Province (No.201903a05020029).

** E-mail: wangyan@ahut.edu.cn

sensor is studied. The accuracy of the algorithm is verified by COMSOL simulations, and the influence of the number of sensors, package thickness ratio and layout on the accuracy of shape reconstruction is investigated. The 600-mm-long aluminum alloy plate is used for the experiment, and after reconstruction, the maximum span relative error is estimated to be 1.203%, and the maximum height relative error is estimated to be 2.802%, which can be the basis for soft robots in the shape perception of complex objects.

According to the sensing theory of FBG, the grating period is changed due to the bending deformation of the sensor. The reflection wavelength of FBG is shown as

$$\lambda_B = 2n_{\text{eff}} \cdot A, \quad (1)$$

where λ_B is the center wavelength of the FBG, n_{eff} is the effective refractive index, and A is the grating period. When the FBG sensor is compressed or stretched, that is, only affected by the axial strain ε , the grating period of the FBG changes, causing the center wavelength to be shifted. Assuming that the external temperature is set as constant, the relationship between the central wavelength drift $\Delta\lambda$ and the axial strain is shown as

$$\Delta\lambda = \lambda_B \cdot (1 - P_\varepsilon) \cdot \varepsilon, \quad (2)$$

where P_ε is the effective elastic-optical coefficient (0.22).

FBG flexible sensors are set to conform ideal deformation conditions. In the flexible bending deformation zone, the inner side of the bend is shortened by compression, while the outer side of the bend is lengthened by tension. Between the two deformation regions of shortening and elongation, there is a fiber layer whose length remains unchanged, that is, the strain variable is zero, which is called the strain neutral layer. The curvature radius of the neutral layer is set as R . When the measured object is deformed, the changes of the neutral layer, compression layer and elongation layer are shown in Fig.1.

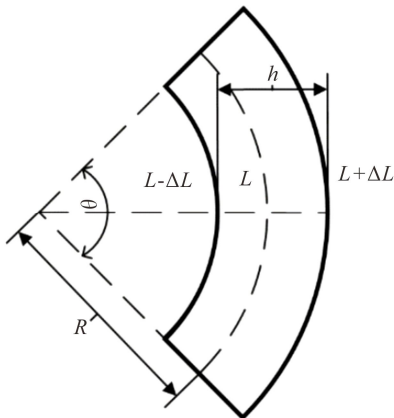


Fig.1 Sensor bending state

The dotted line is called the neutral layer, the length of the element is called L , the change in the length of the structural element is called ΔL , and the central angle corresponding to the circular arc when the element is deformed is called θ . The relationship between bending

radius, bending angle and micro length of FBG flexible sensor is shown as

$$L = R \cdot \theta. \quad (3)$$

The relationship of FBG in bending state is shown as

$$\begin{cases} L - \Delta L = (R - h/2) \cdot \theta \\ L + \Delta L = (R + h/2) \cdot \theta. \\ \varepsilon = \Delta L / L \end{cases} \quad (4)$$

Eq.(5) is obtained by solving the above equations as

$$k = \frac{1}{R} = \frac{2\varepsilon}{h}, \quad (5)$$

where the bending curvature is called k and the thickness of the flexible sensor is called h . According to Eq.(4) and Eq.(5), the relationship between curvature and central wavelength offset can be obtained as

$$k = \frac{\Delta\lambda_B}{\lambda_B \cdot (1 - P_\varepsilon) \cdot h}. \quad (6)$$

For the FBG flexible sensor, λ_B , h and P_ε are constant, therefore bending curvature and the wavelength offset are considered to be a linear relationship. The center wavelength offset of the measuring point of the FBG flexible sensor is detected to obtain the curvature k . This provides a theoretical basis for 2D reconstruction based on curvature information.

Since the curvature data measured by the FBG sensor is discrete, the continuous curvature is obtained by interpolation algorithm, and then the bending curve of the model is reconstructed from the curvature data. The algorithm is based on plane coordinate rotation theory, the knowledge of geometric relation between curve curvature and arc length is combined, the obtained coordinate values are geometrically recurred, the coordinate values of the many points of the whole curve are calculated, then the whole continuous curve is obtained by connecting coordinate points in turn, and the reconstruction of deformation curve is realized^[8].

Fig.2 is the principle of curve reconstruction. First, the initial fixed coordinate system X - Z is established, and the origin is set as O . The tangent of the curve bending at the origin is set to the X -axis, and the Z -axis is perpendicular to X -axis. Several points of equal arc length on the curve are selected as the origin of each moving coordinate system. The X -axis direction of each moving coordinate system is set to point to the tangent of the curve at the origin. To sum up, the relative coordinate value of the next point in the moving coordinate system is obtained through calculation above. The coordinate matrix is rotated as shown in Eq.(7), and the fixed coordinate system is obtained by rotating the moving coordinate system by an angle θ , so the absolute coordinate value of the next point in the fixed coordinate system is calculated.

$$\begin{cases} X = x \sin \theta - z \cos \theta \\ Z = x \cos \theta + z \cos \theta \end{cases} \quad (7)$$

Multiple absolute coordinates in the initial fixed frame X - Z are obtained by repeating the above operation, and these discrete points are connected by straight lines to

reconstruct curved shapes.

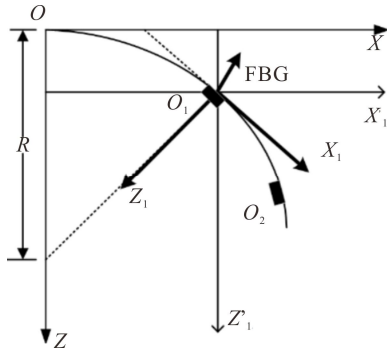


Fig.2 Schematic diagram of shape reconstruction

In practical application, FBG is encapsulated in different degrees, which improves the sensitivity and shear resistance of the sensor because FBG sensors are fragile and easily broken, and also FBG is well protected. If the fiber grating is not encapsulated, the FBG is directly attached to the sensing structure. Due to the limitations of FBG's own characteristics, deformation bending measurements are also limited. Moreover, FBG is directly contacted by the sensing structure, and the two will produce relatively large sliding. The data measured in this way is unreliable. If deformation degree increasing, FBG will be broken^[9]. In this paper, the PDMS material is used to embed the fiber grating, and the relative slippage between the coating layer and silica gel is ignored when the embedded length is greater than 40 mm.

COMSOL simulation software is used to verify the accuracy of the algorithm and explore the reconstruction accuracy influenced by the number of sensors and the layout. The solid mechanics module is selected for the physical field and the steady-state solution is set. The geometric model is drawn as shown in Fig.3. The size of aluminum alloy plate is set as 600 mm×150 mm×2 mm, the outer diameter of optical fiber core and cladding is set as 0.125 mm, and the size of packaging material is set as 80 mm×20 mm×4 mm. The material parameters are shown in Tab.1^[10].

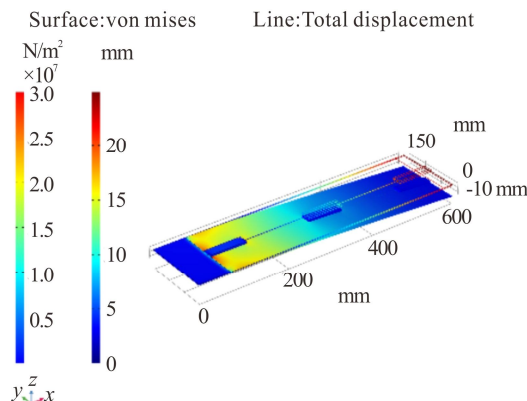


Fig.3 Geometric model and force deformation diagram of aluminum alloy plate in COMSOL

Tab.1 Material parameters of aluminum alloy plate and PDMS

Material	Density (kg/m ³)	Elastic modulus (GPa)	Poisson's ratio
PDMS	1 084	0.01	0.48
Aluminum alloy plate	2 750	71	0.3
Bare fiber	2 203	72	0.17

The left end of the aluminum alloy plate with a length of 70 mm is fixed and the free end is subjected to boundary load with the negative direction of z axis to make the plate surface bend downward. Because the model is relatively simple, the physical field partition is selected. All the constructions are completed for simulation study. The deformation force diagram of aluminum alloy plate is shown in Fig.3.

According to the selected aluminum alloy plate size, three and four FBG flexible sensors are evenly distributed in the middle of the aluminum alloy plate, and the distance between adjacent sensors is set as 225 mm and 150 mm, respectively. The horizontal direction of the aluminum plate without deformation is set as the standard, bending up is set to be positive, bending down is set to be negative, and the directions are indicated by signs of units. Fig.4 shows the shape comparison diagram reconstructed by the number of sensors when the boundary load of 10 N is applied to the free end of the aluminum alloy plate through the experiment. The relative errors of length and height are calculated by the three FBG flexible sensors are 1.160 9% and 8.292 4%, respectively, and the relative errors of length and height are calculated by the four FBG flexible sensors are 1.171 7% and 5.702 6%, respectively (see Tab.2). In conclusion, the aluminum alloy plate shape with four FBG flexible sensors is considered to have better reconstruction effect and higher reconstruction accuracy. Therefore, four sensors are used to discuss the influence of layout on shape reconstruction in this paper.

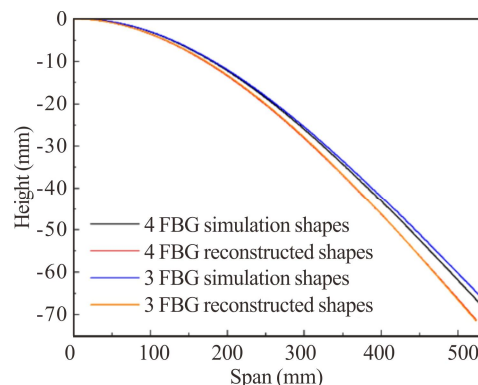


Fig.4 Comparison of sensor number and shape reconstruction when 10 N boundary load is applied

Tab.2 Lengths and heights from COMSOL simulation and algorithm reconstruction for different numbers of sensors

	COMSOL simulation (nm)	Algorithm reconstruction (nm)	Absolute error (nm)	Relative error (%)
The length of three sensors	529.814 2	523.663 8	6.150 4	1.160 9
The length of four sensors	529.807 4	523.599 7	6.207 7	1.171 7
Height of three sensors	-65.822 6	-71.280 9	5.458 3	8.292 4
Height of four sensors	-67.653 4	-71.511 4	3.858 0	5.702 6

In the silicone packaging base material, the precision of aluminum alloy plate shape reconstruction is affected by the position of FBG flexible sensor. FBG sensors are packaged in proportion positions of 9: 1, 8: 2, 7: 3, 6: 4 and 5: 5 in silica gel base material with thickness of 4 mm. In COSMOL simulation, five groups of aluminum alloy plate geometric models are established, and four FBG flexible sensors are set on each group of aluminum alloy plate, each with the same size. Field point probes are set at the grid position of each FBG flexible sensor. The stress data of the field point probe positions in five groups of finite element simulation are imported into MATLAB. The shape of plate is reconstructed by coordinate transformation algorithm and compared with the COMSOL simulation shape.

As shown in Fig.5, as the upper and lower ratio of sensor package position is gradually reduced, the relative error of reconstructed shape is also reduced. When the ratio between the FBG sensor and the silica gel surface is set as 5: 5, the relative error of plate structure reconstruction is calculated to be 2.260 8%. In conclusion, the FBG flexible sensor aluminum alloy plate with a ratio of 5: 5 in the silica gel packaging position is selected for better shape reconstruction effect and higher reconstruction accuracy.

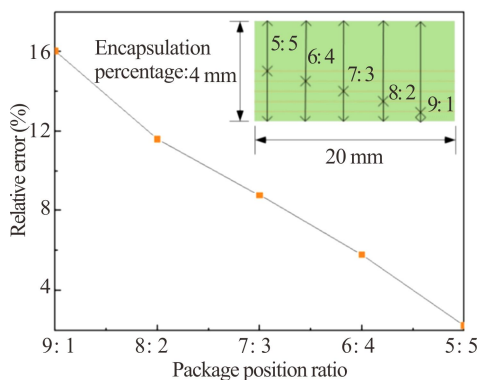


Fig.5 Relative errors of five groups of plate structure shape reconstruction with different position sensors

As shown in Fig.3, when aluminum alloy plate is bent, the stress and displacement are different at different points. Therefore, four sensors are arranged on the aluminum alloy surface according to the law of stress distribution, and the effect of sensor layout on shape reconstruction is discussed, as shown in Fig.6. The sensors are distributed in seven ways, as shown in Tab.3.



Fig.6 Four sensors distributed on the aluminum alloy plate

Tab.3 Distribution patterns of four sensors at different intervals

Layout	a (mm)	b (mm)	c (mm)
1	90	100	260
2	110	120	220
3	130	140	180
4	150	150	150
5	180	140	130
6	220	120	110
7	260	100	90

As shown in Fig.7, it is not difficult to find that the four sensors are arranged on the aluminum alloy plate according to the seven groups of different layouts in Tab.1. FBG layouts are selected from 1 to 7. The absolute error of FBG4 sensor and terminal reconstruction is minimal when layout 7 is selected, and measured data are 4.752 mm and 4.152 mm, respectively. According to the same analysis, when layout 7 is selected, FBG1, FBG2, FBG3, and FBG4 have the smallest relative errors in sensor and terminal reconstruction, which are 30.106%, 6.049%, 6.197%, 6.269% and 4.669%, respectively. To sum up, four FBG flexible sensors with 260 mm, 100 mm, and 90 mm spacing are selected to achieve the best shape reconstruction and the highest reconstruction accuracy.

The temperature is set as 24 °C. Curvature calibration experiments are carried out on four FBG flexible sensors successively under six different bending curvatures of 0 m⁻¹, 3.61 m⁻¹, 5.13 m⁻¹, 6.30 m⁻¹, 7.31 m⁻¹ and 8.20 m⁻¹. The demodulation equipment used in the experiment is manufactured by MOI Company, models for SI155, where the resolution is 0.1 pm, the accuracy is 1 pm, and the sampling frequency is set as 1 000 Hz. The MOI demodulation instrument has four parallel optical channels, which can be used independently without affecting each other. The demodulation wavelength ranges are 1 520—1 580 nm, 1 500—1 560 nm and 1 460—1 620 nm.

The central wavelengths of the four fiber gratings selected in this paper are 1 549.94 nm, 1 544.93 nm, 1 545.90 nm and 1 554.90 nm, respectively. In order to reduce the experimental error, each FBG is calibrated four times in the same curvature, and the average value of the central wavelength offset is taken as the calibration data under the curvature. Wavelength migration of FBG flexible sensor under different curvatures is shown in Fig.8.

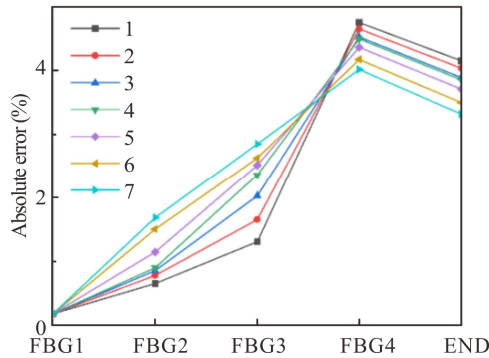


Fig.7 Line chart of absolute error of sensor board structure and shape reconstruction with different layouts

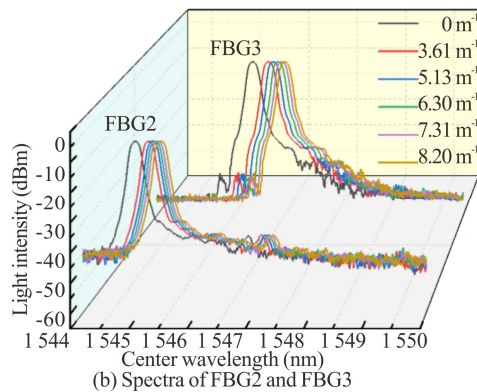
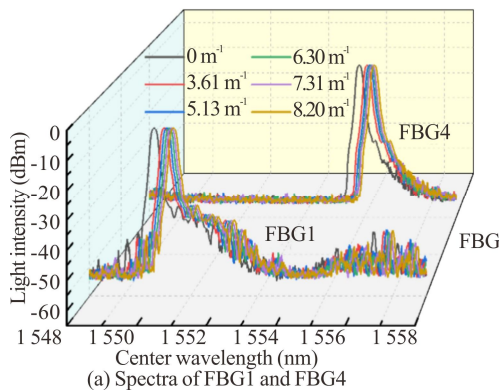


Fig.8 Central wavelength shifts of four FBGs under different curvatures

As shown in Fig.8, according to the central wavelength shifts of the four FBGs at different curvatures, the wavelength changes of each measuring point at different

curvatures are calculated, and the least square method is used for linear fitting. The relation between wavelength offset and curvature of four FBG flexible sensors is shown in Fig.9. The determination coefficients R are calculated as 0.996 0, 0.996 2, 0.997 6 and 0.995 6, respectively. The total wavelength shifts and average sensitivities of the four FBGs are shown in Tab.4.

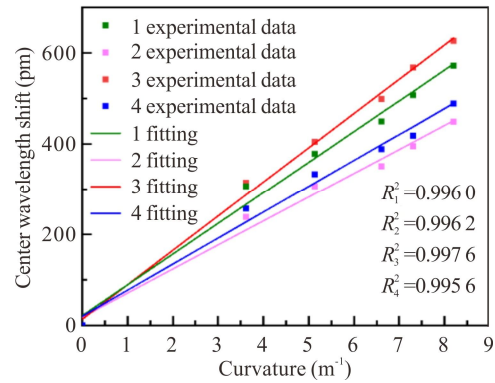


Fig.9 Relationship between the center wavelength shift and the curvature for the four FBGs

Tab.4 Total wavelength shifts and average sensitivities of the four FBGs

Sensor	Average sensitivity (pm/m ⁻¹)	Center wavelength (nm)	Total wavelength shift (nm)
FBG1	68.584	1 549.94	0.570 4
FBG2	61.712	1 544.93	0.474 8
FBG3	71.978	1 545.90	0.604 3
FBG4	61.712	1 554.90	0.506 5

The experimental system as shown in Fig.10 is established in this paper. The aluminum alloy plate of 600 mm×150 mm×2 mm is selected to fix one end of the plate on the iron frame. FBG flexible sensors are distributed in the middle of the plate according to layout 7. The free end of the plate is deformed by loading weights of different weights, the strain of the sensor is measured by demodulation instrument, and the measured data are reconstructed by plane rotation coordinate algorithm. The span and height at the end of aluminum alloy plate are measured by laser displacement sensor. The two are compared to analyze the accuracy of reconstruction algorithm.

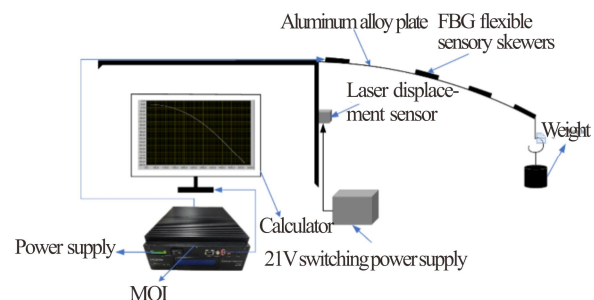


Fig.10 Experimental setup for FBG flexible sensor shape reconstruction

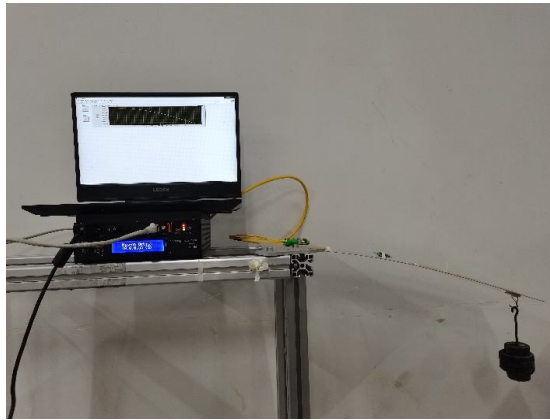


Fig.11 Bending diagram and reconstruction

According to layout 7, four FBG flexible sensors are distributed on the surface of the aluminum alloy plate. One end of the aluminum alloy plate is fixed, and weights of 100 g, 300 g, 500 g, 700 g and 1 000 g are applied to the other end, respectively. The reconstructed plate section is shown in Fig.12. The end span and height displacement of aluminum alloy plate under five different weights are measured as shown in Tab.5. The maximum relative error of the end span is 1.203%, and the

maximum relative error of the end height is 2.802%.

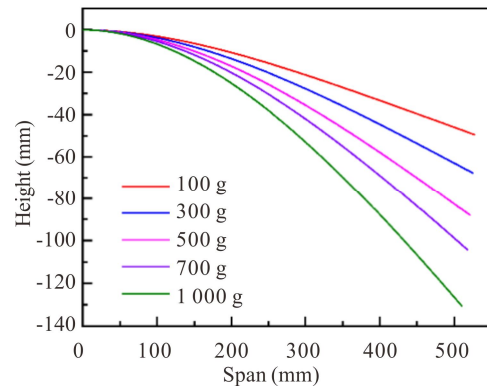


Fig.12 Reconstruction results of plate section shape

In this paper, the curvature measurement of fiber grating is analyzed theoretically. The FBG sensor is packaged into flexible sensor by PDMS material to explore the influence of the number, embedment ratio and layout of sensors on the reconstruction accuracy of object shape. COMSOL simulation software is used to verify the accuracy of the algorithm. The influence of the number of sensors and 7 layouts on the relative error of aluminum alloy plate shape

Tab.5 Terminal displacement and relative error

Weight (g)	Height relative error (%)	Relative span error (%)	Test end height (mm)	Test end span (mm)	Reconstruction end height (mm)	Reconstructed end span (mm)
100	2.802	0.289	50.9	528.6	49.47	527.07
300	1.659	0.353	68.7	526.5	67.56	524.64
500	0.506	0.537	88.3	523.8	87.85	520.99
700	1.237	0.682	105.4	520.9	104.1	517.35
1000	1.562	1.203	128.5	516.2	130.51	509.99

reconstruction is discussed. Simulation results show that for the aluminum alloy plate, the relative error of shape reconstruction is the smallest and the reconstruction accuracy is the highest when four sensors are used with 260 mm, 100 mm and 90 mm intervals, respectively. Then, the curvature calibration of FBG flexible sensor is carried out through the relationship between curvature and center wavelength migration, and the corresponding experimental system is built. The same spacing scheme is adopted and the weights of 100 g, 300 g, 500 g, 700 g and 1 000 g are applied to one end of the aluminum alloy plate, and the maximum relative error of shape reconstruction span is 1.203%. The maximum relative error of height is 2.802%, which is consistent with the simulation results. The research results provide an application basis for soft robot shape detection. In this paper, experiments are only carried out on the aluminum alloy surface, and more complex object shape reconstruction will be further

studied in the future.

Statements and Declarations

The authors declare that there are no conflicts of interest related to this article.

References

[1] YAN J, LI W, JIANG S M, et al. Shape perception and three-dimensional reconstruction technology of plate structure based on fiber Bragg grating sensor[J]. Chinese journal of lasers, 2020, 47(11): 231-240.
 [2] GUO R Y, BAO Y. Research progress on wearable piezoresistive strain sensors based on two-dimensional conductive materials/flexible polymer composites[J]. Fine chemicals, 2021, 38(04): 649-661.
 [3] XU D C, GUO X H. Design and application of capacitive

- slip sensor[J]. *Transducer and microsystem technologies*, 2015, 34(11): 85-88.
- [4] GUO Y X, YANG Y H, XIONG L. Double-layer orthogonal fiber Bragg gratings flexible shape sensing technology[J]. *Optics and precision engineering*, 2021, 29(10): 2306-2315.
- [5] YANG M, LIU Q D. Movement detection in soft robotic gripper using sinusoidally embedded fiber optic sensor[J]. *Sensors*, 2020, 20(5): 1312.
- [6] ISMAIL N N, SHARBIRIN A S. Novel 3D-printed biaxial tilt sensor based on fiber Bragg grating sensing approach[J]. *Sensors and actuators A physical*, 2021, 330: 112864.
- [7] GROVES R M, NAZEER N, WANG X R. Sensing, actuation, and control of the SmartX prototype morphing wing in the wind tunnel[J]. *Actuators*, 2021, 10(6): 107.
- [8] ZHUANG W, SUN G K, LI H. FBG based shape sensing of a silicone octopus tentacle model for soft robotics[J]. *Optik-international journal for light and electron optics*, 2018, 165: 7-15.
- [9] WANG Y, QIN N, LIU J H. Performance test of temperature and pressure flexible sensor based on optical fiber Bragg grating[J]. *Chinese journal of scientific instrument*, 2019, 40(03): 93-98.
- [10] ZHANG S, TAO W, LEE C. Silicon nanowires embedded pressure sensor with annularly grooved diaphragm for sensitivity improvement[C]//IEEE Ninth International Conference on Intelligent Sensors, April 21-24, 2014, Singapore. New York: IEEE, 2014: 14378510.